Acta Cryst E CRYSTALLOGRAPHIC COMMUNICATIONS

ISSN 2056-9890

3-{(*E*)-[4-(4-Hydroxy-3-methoxyphenyl)butan-2-ylidene]amino}-1-phenylurea: crystal structure and Hirshfeld surface analysis

Ming Yueh Tan,[a] Karen A. Crouse,[b,c] Thahira B. S. A. Ravoof,[b]‡ Mukesh M. Jotani[d] and Edward R. T. Tiekink[e]*

[a]Department of Physical Science, Faculty of Applied Sciences, Tunku Abdul Rahman, University College, 50932 Setapak, Kuala Lumpur, Malaysia, [b]Department of Chemistry, Faculty of Science, Universiti Putra Malaysia, 43400, UPM Serdang, Selangor Darul Ehsan, Malaysia, [c]Department of Chemistry, St. Francis Xavier University, PO Box 5000, Antigonish, NS B2G 2W5, Canada, [d]Department of Physics, Bhavan's Sheth R. A. College of Science, Ahmedabad, Gujarat 380001, India, and [e]Research Centre for Crystalline Materials, School of Science and Technology, Sunway University, 47500 Bandar Sunway, Selangor Darul Ehsan, Malaysia. *Correspondence e-mail: edwardt@sunway.edu.my

Received 27 November 2017
Accepted 2 December 2017

Edited by W. T. A. Harrison, University of Aberdeen, Scotland

‡ Additional correspondence author, e-mail: thahira@upm.edu.my

Keywords: crystal structure; urea derivative; hydrogen bonding; Hirshfeld surface analysis.

CCDC reference: 926756

Supporting information: this article has supporting information at journals.iucr.org/e

Two independent molecules (*A* and *B*) comprise the asymmetric unit of the title compound, $C_{18}H_{21}N_3O_3$. The urea moiety is disubstituted with one amine being linked to a phenyl ring, which is twisted out of the plane of the CN_2O urea core [dihedral angles = 25.57 (11) (*A*) and 29.13 (10)° (*B*)]. The second amine is connected to an imine (*E* conformation), which is linked in turn to an ethane bridge that links a disubstituted benzene ring. Intramolecular amine-N—H···N(imine) and hydroxyl-O—H···O(methoxy) hydrogen bonds close *S*(5) loops in each case. The molecules have twisted conformations with the dihedral angles between the outer rings being 38.64 (81) (*A*) and 48.55 (7)° (*B*). In the crystal, amide-N—H···O(amide) hydrogen bonds link the molecules *A* and *B* *via* an eight-membered $\{\cdots HNCO\}_2$ synthon. Further associations between molecules, leading to supramolecular layers in the *ac* plane, are hydrogen bonds of the type hydroxyl-O—H···N(imine) and phenylamine-N—H···O(methoxy). Connections between layers, leading to a three-dimensional architecture, comprise benzene-C—H···O(hydroxy) interactions. A detailed analysis of the calculated Hirshfeld surfaces shows molecules *A* and *B* participate in very similar intermolecular interactions and that any variations relate to conformational differences between the molecules.

1. Chemical context

Semicarbazones belong to the general class of molecules termed Schiff bases and are prepared from condensation of semicarbazides with aldehydes/ketones. They have attracted considerable attention due to their wide spectrum of biological activities, including anti-convulsant (Pandey & Srivastava, 2010), anti-tubercular (Sriram *et al.*, 2004), anti-cancer (Ali *et al.*, 2012) and anti-microbial (Beraldo & Gambino, 2004). Actually, they have been investigated extensively for their anti-convulsant properties with 4-(4-fluorophenoxy)benzaldehyde semicarbazone, in particular, attracting attention as a potent anti-epileptic drug over the past 15 years (Pandeya, 2012). Recently, the crystal structures of related chalcone-derived thiosemicarbazones and their transition metal complexes have been reported (Tan *et al.*, 2015, 2017). In this contribution, aryl semicarbazide is introduced with vanillylacetone, which led to the formation of the title compound. Vanillylacetone is one of the active components of ginger and possesses strong anti-oxidant and chemopreventive

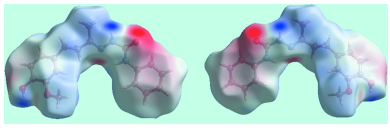

properties (Kıyak *et al.*, 2015). The structural elucidation of such compounds has not been extensively investigated. In order to redress this, herein the crystal and molecular structures of the title compound, (I), are described along with an analysis of the calculated Hirshfeld surface in order to ascertain more details of the supramolecular association operating in the crystal.

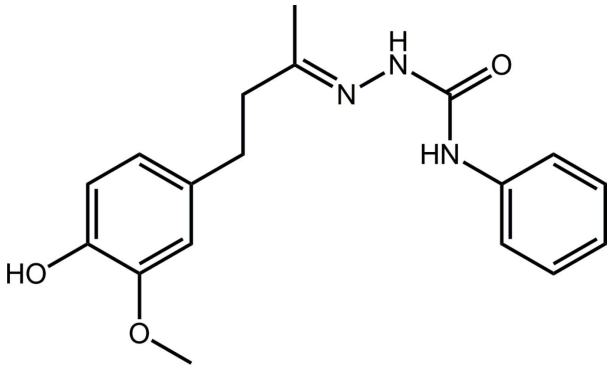

2. Structural commentary

Two independent molecules, *A* and *B*, comprise the asymmetric unit of (I) and these are shown in Fig. 1. Each molecule features a disubstituted urea molecule with one amine group connected to a phenyl ring and the other linked to a disubstituted imine group, with the longer side-chain carrying an ethane chain terminating with a disubstituted benzene ring. The four atoms comprising the urea core are strictly planar with an r.m.s. deviation of 0.0041 Å [0.0043 for the O4-molecule, molecule *B*]. The phenyl ring is inclined to this plane, forming a dihedral angle of 25.57 (11)° [29.13 (10)° for molecule *B*]. Intramolecular N—H···N hydrogen bonds are found within the urea residues, Table 1. A significant kink in the molecule occurs in the ethane bridge, as seen in the value of −157.88 (16)° for the C8—C9—C10—C11 torsion angle [C26—C27—C28—C29 = 162.93 (17)° for *B*]. As a result, the molecule is twisted with the terminal rings inclined to each other, forming a (C2–C7)/(C11–C16) dihedral angle of 38.64 (8)° [(C20–C25)/(C29–C34) = 48.55 (7)° for *B*]. The latter represents the major difference between molecules *A* and *B*, as illustrated in the overlay diagram shown in Fig. 2. In each of the disubstituted benzene rings, the hydroxyl-H atom is orientated to allow the formation of intramolecular O—

Table 1
Hydrogen-bond geometry (Å, °).

*Cg*1, *Cg*2 and *Cg*3 are the centroids of the C2–C7, C29–C34 and C20–C25 rings, respectively.

D—H···*A*	*D*—H	H···*A*	*D*···*A*	*D*—H···*A*
N1—H1*N*···N3	0.86 (2)	2.18 (2)	2.635 (2)	113 (2)
N4—H4*N*···N6	0.86 (2)	2.23 (2)	2.637 (2)	109 (1)
O3—H3*O*···O2	0.84 (2)	2.29 (3)	2.660 (2)	107 (2)
O6—H6*O*···O5	0.84 (2)	2.28 (2)	2.663 (2)	108 (2)
O3—H3*O*···N6^{i}	0.84 (2)	2.19 (2)	2.994 (2)	161 (2)
O6—H6*O*···N3^{ii}	0.84 (2)	2.22 (2)	3.013 (2)	157 (2)
N2—H2*N*···O4^{iii}	0.88 (2)	2.01 (2)	2.873 (2)	170 (2)
N4—H4*N*···O2^{i}	0.86 (2)	2.54 (2)	3.390 (2)	167 (2)
N5—H5*N*···O1^{iv}	0.88 (2)	2.04 (2)	2.900 (2)	169 (2)
C33—H33···O6^{v}	0.95	2.54	3.212 (2)	128
C15—H15···O3^{vi}	0.95	2.63	3.166 (2)	113
C33—H33···O6^{i}	0.95	2.54	3.212 (2)	128
C10—H10*A*···*Cg*1^{vii}	0.99	2.80	3.774 (2)	168
C18—H18*A*···*Cg*2^{ii}	0.98	2.66	3.603 (4)	161
C28—H28*B*···*Cg*3^{viii}	0.99	2.75	3.720 (2)	166

Symmetry codes: (i) $-x+1, -y+1, -z+1$; (ii) $-x+1, -y, -z+1$; (iii) $-x+\frac{3}{2}, y+\frac{1}{2}, -z+\frac{1}{2}$; (iv) $-x+\frac{3}{2}, y-\frac{1}{2}, -z+\frac{1}{2}$; (v) $-x+1, -y-1, -z+1$; (vi) $-x, -y+2, -z$; (vii) $x, y+1, z$; (viii) $x, y-1, z$.

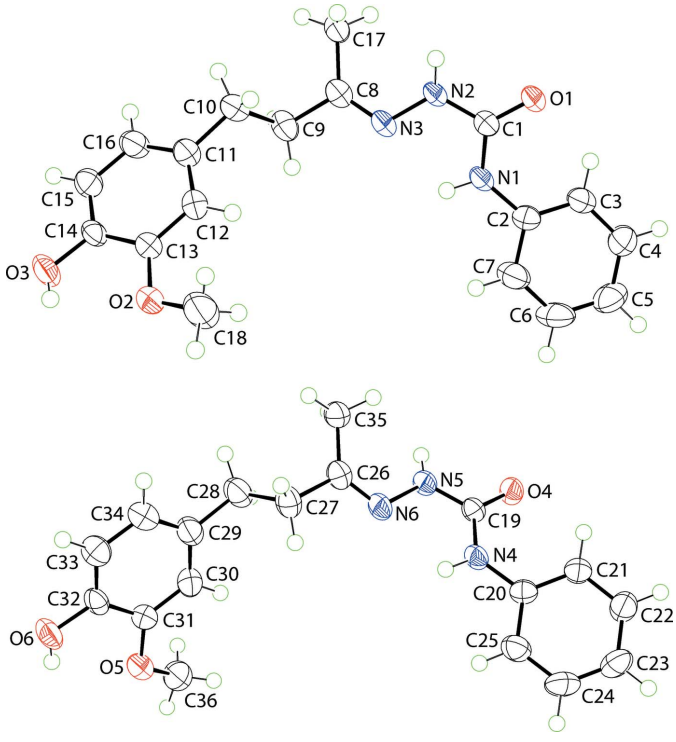

Figure 1
The molecular structures of the two independent molecules comprising the asymmetric unit of (I), showing the atom-labelling scheme and displacement ellipsoids at the 70% probability level.

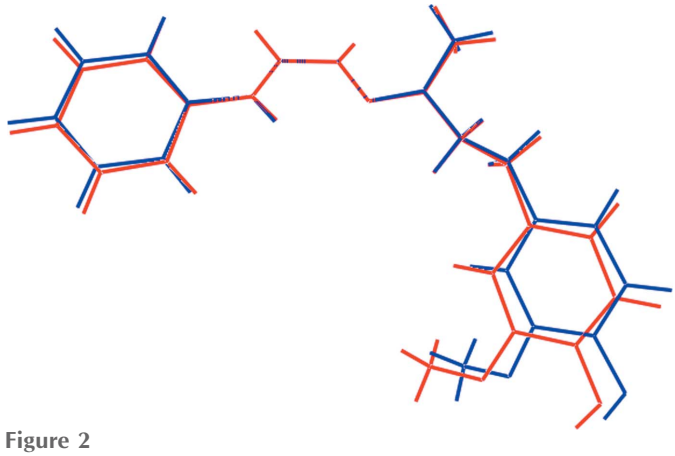

Figure 2
Overlay diagram for (I), with the O1-molecule (red image) and O4-molecule (blue image) superimposed so that the urea residues are coincident.

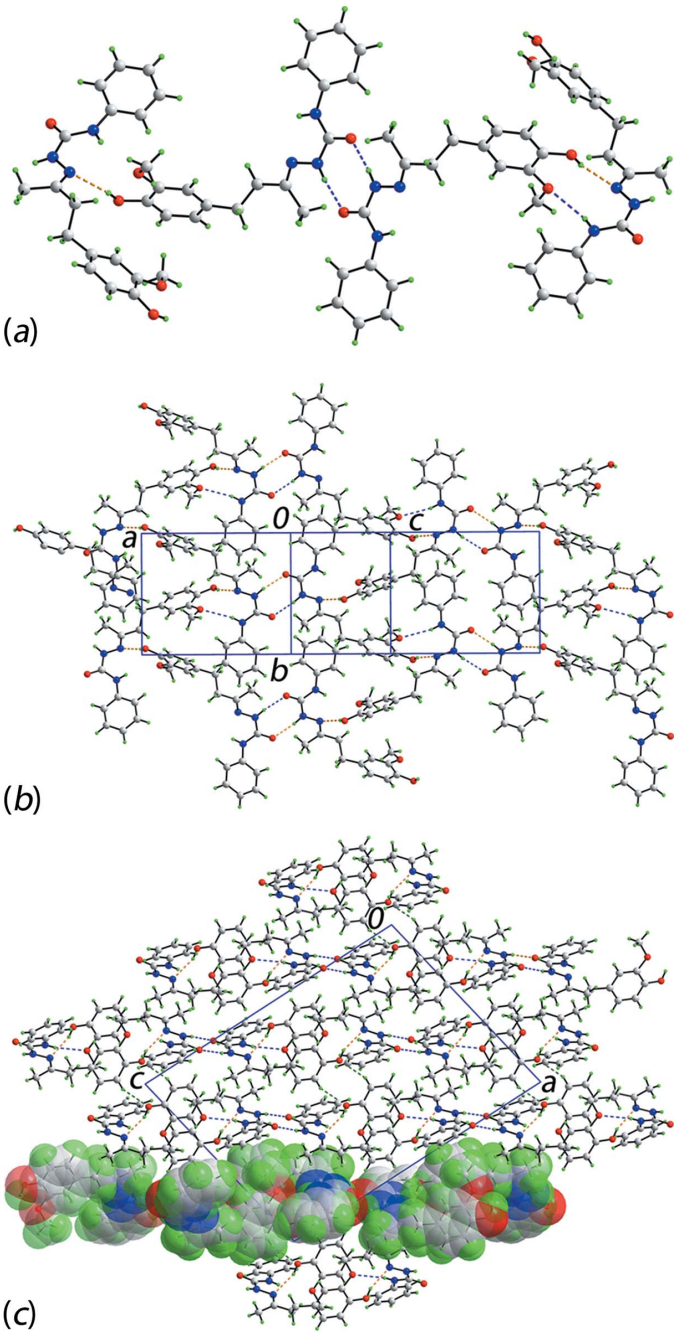

Figure 3
The molecular packing in (I): (*a*) a detail of the supramolecular association sustained by O—H···N and N—H···O hydrogen bonding, shown as orange and blue dashed lines, respectively, (*b*) a view of the supramolecular layer in the *ac* plane, and (*c*) a view of the unit-cell contents shown in projection down the *b* axis. The C—H···O interactions are shown as green dashed lines, and one layer is highlighted in space-filling mode.

H···O hydrogen bonds with the methoxy-O atom, Table 1. The conformation about the imine bond [N3═C8 = 1.281 (2) and N6═C26 = 1.276 (2) Å] is *E* in each molecule. Finally, each of the methoxy substituents is twisted out of the plane of the ring to which it is bonded [C18—O2—C13—C12 = 11.7 (3) and C36—O5—C31—C30 = −16.5 (3)°].

Table 2
Summary of short interatomic contacts (Å) in (I).

Contact	Distance	Symmetry operation
H3···H21	2.16	$\frac{3}{2}-x,-\frac{1}{2}+y,\frac{1}{2}-z$
H28*A*···H35*A*	2.24	$\frac{5}{2}-x,-\frac{1}{2}+y,\frac{1}{2}-z$
O1···H22	2.50	$\frac{3}{2}-x,-\frac{1}{2}+y,\frac{1}{2}-z$
O2···H27*B*	2.56	$1-x,1-y,1-z$
O3···H15	2.63	$-x,2-y,1-z$
O3···C15	3.166 (2)	$-x,2-y,1-z$
O3···H23	2.58	$1-x,2-y,1-z$
O4···H16	2.58	$1+x,-1+y,z$
O5···H9*A*	2.46	$1-x,-y,1-z$
C6···H10*A*	2.63	$x,-1+y,z$
C15···H36*C*	2.55	$1-x,1-y,1-z$
C16···H36*C*	2.80	$1-x,1-y,1-z$
C24···H28*B*	2.63	$x,1+y,z$
C32···H18*A*	2.76	$1-x,-y,1-z$
C33···H18*A*	2.62	$1-x,-y,1-z$
C34···H18*A*	2.78	$1-x,-y,1-z$
C35···H18*B*	2.71	$\frac{1}{2}+x,\frac{1}{2}-y,-\frac{1}{2}+z$
C36···H9*A*	2.80	$1-x,-y,1-z$
C6···C6	3.210 (3)	$1-x,-y,1-z$
C24···C24	3.300 (3)	$2-x,1-y,1-z$

3. Supramolecular features

Conventional O—H···N and N—H···O hydrogen bonding features significantly in the molecular packing of (I), Table 1, and this is highlighted in Fig. 3*a*. The two molecules comprising the asymmetric unit associate *via* an eight-membered amide synthon, {···OCNH}$_2$. The hydroxy-O—H groups at each end of the dimeric aggregate hydrogen bond to an imine-N atom of the other independent molecule. The hydroxyl-O3—H···N6(imine) interaction is incorporated within a 10-membered {···HOC$_2$O···HNCNN} heterosynthon owing to the formation of a relatively weak phenylamine-N4—H···O2(methoxy) hydrogen bond. The putative phenylamine-N1—H···O5(methoxy) hydrogen bond is beyond the standard limits (Spek, 2009) as the H···O separation is 2.73 Å. As seen in Fig. 3*b*, these hydrogen bonds extend laterally to from an array in (101). The most obvious connections between the supramolecular layers are of the type benzene-C—H···O(hydroxyl), which occur between centrosymmetrically related O6-benzene rings. A view of the unit-cell contents highlighting the stacking of layers is shown in Fig. 3*c*. Other C—H···O and several C—H···π interactions occur in the crystal but within the layers stabilized by hydrogen bonding. These and other weak interactions are discussed in more detail in *Analysis of the Hirshfeld surface* (§4).

4. Analysis of the Hirshfeld surface

The Hirshfeld surface was calculated for the individual O1- and O4-molecules in (I), *i.e.* molecules *A* and *B*, and for overall (I) in accord with a recent report on a related molecule (Tan *et al.*, 2017). These calculations provide additional information about the influence of weak intermolecular C—H···O and C—H···π interactions, Table 1, along with short

Table 3
Percentage contributions of interatomic contacts to the Hirshfeld surface for the O1-molecule, the O4-molecule and for overall (I).

Contact	Percentage contribution		
	O1-molecule	O4-molecule	(I)
H···H	49.5	49.4	48.7
O···H/H···O	16.4	17.5	17.8
N···H/H···N	7.4	7.3	7.7
C···H/H···C	26.3	25.7	25.5
C···C	0.1	0.1	0.1
O···O	0.2	0.0	0.1
C···O/O···C	0.1	0.0	0.1

interatomic H···H, C···H/H···C and O···H/H···O contacts, Table 2, on the molecular packing in the crystal.

The bright-red spots appearing near the hydroxyl-H3*O* and H6*O*, and imine-N3 and N6 atoms on the Hirshfeld surfaces mapped over d_{norm} shown with labels '*1*' and '*2*' in Fig. 4 represent the donors and acceptors of intermolecular hydroxyl-O—H···N(imine) hydrogen bonds, respectively, Table 1. In the same way, the prominent red regions near the amide-H2*N* and H5*N*, and amide-O1 and O4 atoms, *i.e.* '*3*' and '*4*' in Fig. 4, indicate their participation in the intermolecular N—H···O hydrogen bonds between the symmetry-related independent molecules, Table 1. The donors and acceptors of comparatively weak intermolecular N—H···O and C—H···O interactions summarized in Table 1 are viewed as faint-red spots near the respective atoms on d_{norm}-mapped Hirshfeld surfaces with labels '*5*–*7*' in Fig. 4.

The presence of diminutive red spots viewed near phenyl atoms C6 in Fig. 4*a* and C24 in Fig. 4*b*, of the independent molecules, respectively, reflect short interatomic edge-to-edge C···C contacts, Table 2, although they contribute a very low contribution, *i.e.* 0.1%, to the Hirshfeld surface owing to the absence of π–π stacking between aromatic rings in the crystal, Table 3. The faint-red spots appearing near the labelled H10*A*, H18*A*, C28, C6, C33 and C24 atoms in the images of Fig. 4

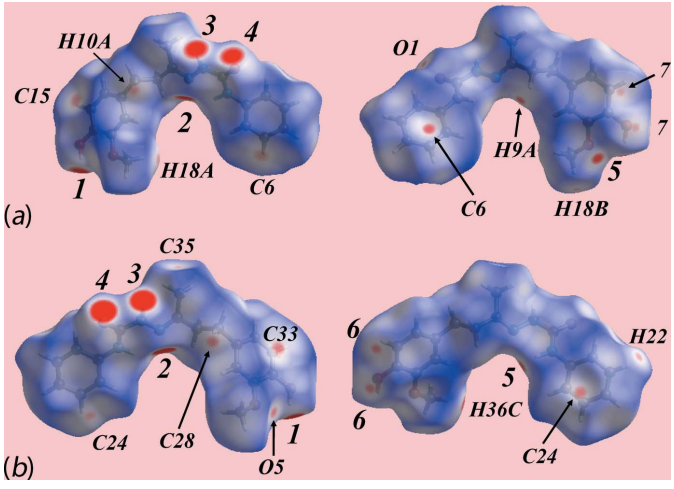

Figure 4
Views of the Hirshfeld surface for (I) mapped over d_{norm} in the ranges (*a*) −0.150 to +1.462 au for the O1-containing molecule and (*b*) −0.215 to + 1.462 au for the O4-molecule.

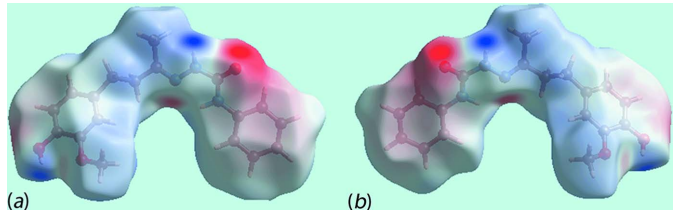

Figure 5
Views of the Hirshfeld surface for (I) mapped over the electrostatic potential in the range −0.103 to + 0.141 au for the (*a*) O1-containing molecule and (*b*) the O4-molecule. The red and blue regions represent negative and positive electrostatic potentials, respectively.

represent their participation in short interatomic C···H/H···C contacts, Table 2, and confirm the influence of the intermolecular C—H···π interactions, Table 1, in the crystal. In addition to these short interatomic C···H/H···C contacts, the faint-red spots near the C15 O1, H9*A* and H18*B* atoms,

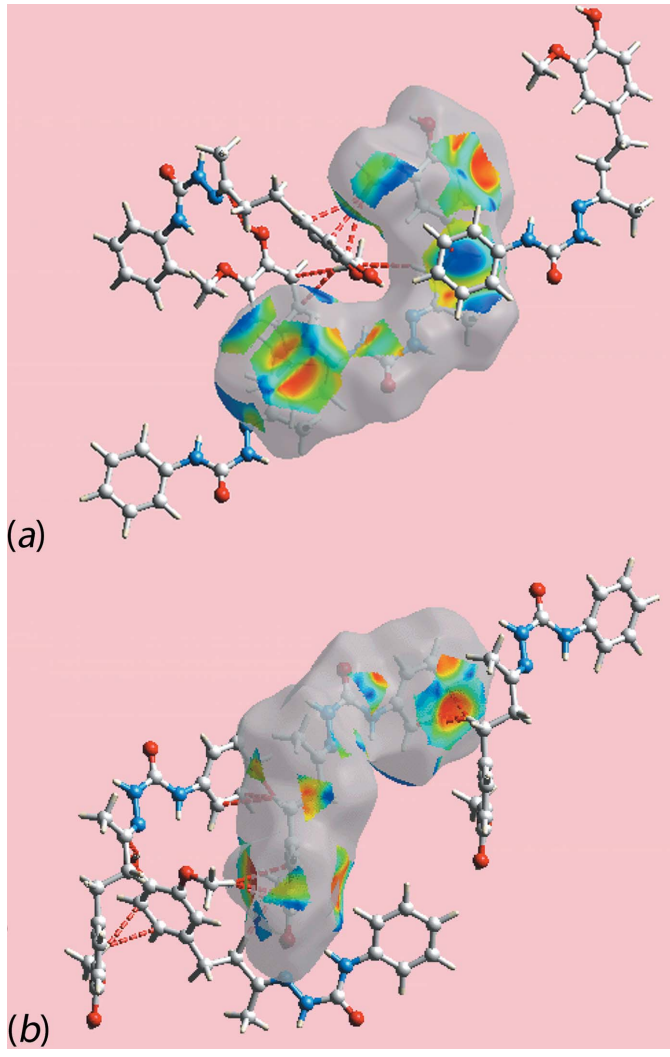

Figure 6
Views of the shape-indexed Hirshfeld surfaces about reference molecules highlighting dominant short interatomic C—H/H—C and C—H···π/π···H—C interactions for the (*a*) O1-containing molecule and (*b*) the O4-molecule.

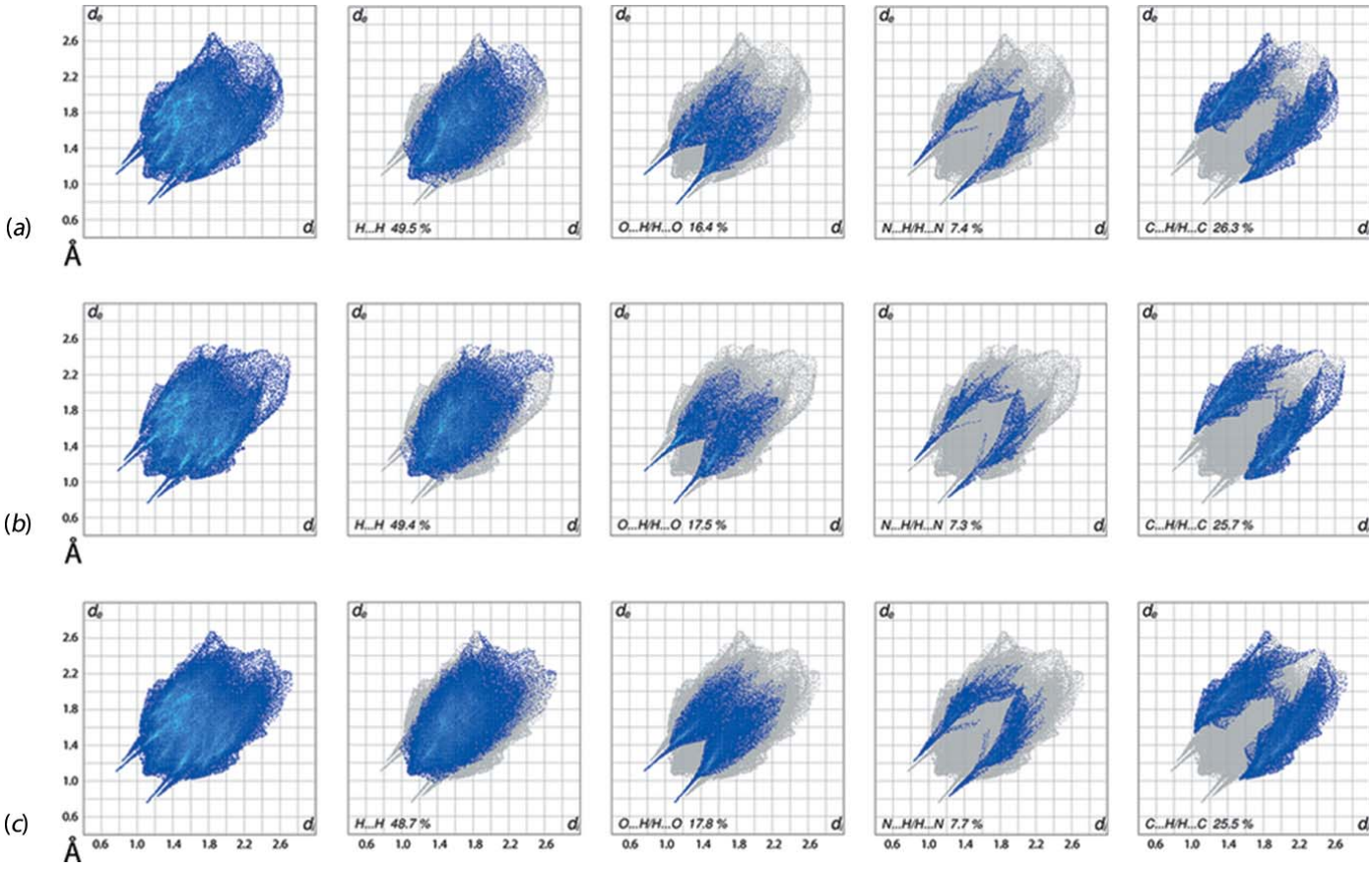

Figure 7
The full two-dimensional fingerprint plot and those delineated into H···H, O···H/H···O, N···H/H···N and C···H/H···C contacts for the (*a*) O1-containing molecule, (*b*) the O4-molecule and (*c*) (I).

Fig. 4*a*, and O5, C35, H22 and H36*C* atoms, Fig. 4*b*, indicate the contributions from the additional short interatomic C···H/H···C and O···H/H···O contacts, Table 2, to the molecular packing.

On the Hirshfeld surfaces mapped over the electrostatic potential for the independent molecules of (I), Fig. 5, the donors and acceptors of intermolecular interactions are represented with blue and red regions corresponding to positive and negative electrostatic potentials, respectively. The views of Hirshfeld surfaces about reference independent molecules of (I) mapped within the shape-index property, Fig. 6, highlight the short interatomic C···H/H···C and C—H···π/π···H—C contacts operating in the crystal.

It is clear from the overall two-dimensional fingerprint plots for each independent molecule and for the entire asymmetric unit of (I) shown in Fig. 7 that the individual molecules have common features in their intermolecular O—H···N, N—H···O and C—H···π interactions. The small differences in the distribution of points in the fingerprint plots delineated into H···H, O···H/H···O, N···H/H···N and C···H/H···C contacts (McKinnon *et al.*, 2007) in Fig. 7, are ascribed to the commented upon (§3) conformational differences, *i.e.* the twisting of the methoxy substituents on the respective benzene rings and the inclination of these benzene rings with respect to the ethane bridges.

The fingerprint plot delineated into H···H contacts for molecules *A* and *B* have almost the same percentage contribution to their respective Hirshfeld surfaces, Table 3, and the distinct distributions in the upper regions of the plots are due to the contributions from hydrogen atoms of their respective disubstituted benzene rings to the surfaces of molecules *A* and *B*. The single short peaks at $d_e + d_i \sim 2.1$ Å in the delineated plots for both the molecules indicate the involvement of hydrogen atoms of both in short interatomic H···H contacts, Table 2. The intermolecular N—H···O and O—H···N hydrogen bonds in the crystal are characterized as the pairs of spikes with their tips at $d_e + d_i \sim 2.0$ Å (inner region) and at ~ 2.2 Å (outer region) in the fingerprint plots delineated into O···H/H···O and N···H/H···N contacts, respectively. The forceps-like distribution of points linked with the donor spike for molecule *A* and the acceptor spike for molecule *B* at $d_e + d_i \sim 2.5$ Å in the fingerprint plots delineated into O···H/H···O contacts are due to weak intermolecular C—H···O interactions and the short interatomic contacts summarized in Table 2. The asymmetric forceps-like distribution of points with the tips at $d_e + d_i \sim 2.6$ Å in the acceptor and donor regions of fingerprint plots delineated into C···H/H···C contacts for molecules *A* and *B*, respectively, represent the involvement of these atoms in the short interatomic C···H/H···C contacts, Table 2, whereas the intermolecular C—H···π

interactions are viewed as the forceps-like tips at $d_e + d_i \sim$ 2.7 Å in the donor and acceptor regions of molecules *A* and *B*, respectively. The other C···O/O···C, O···O and C···C interatomic contacts summarized in Table 3, having only small contributions to the Hirshfeld surface, have negligible directional impact on the molecular packing.

5. Database survey

There are no direct precedents for the structure of (I) in the crystallographic literature (Groom *et al.*, 2016). However, there are several precedents for the phenylsemicarbazone residue with the imine-carbon atom incorporated within an all-carbon ring (Groth, 1980; Hoek van den *et al.*, 1980), as exemplified in the cyclodecane derivative (II) (Groth, 1980; Hoek van den *et al.*, 1980), see Scheme 2 for the chemical diagram of (II). More exotic derivatives with cyclic residues at both ends of the semicarbazone core are also known (Behenna *et al.*, 2011; Ma *et al.*, 2014), as exemplified by (III) (Ma *et al.*, 2014), Scheme 2.

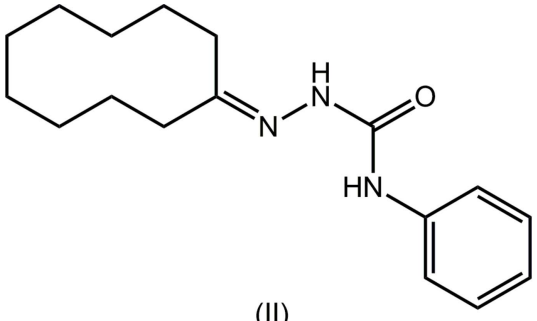

(II)

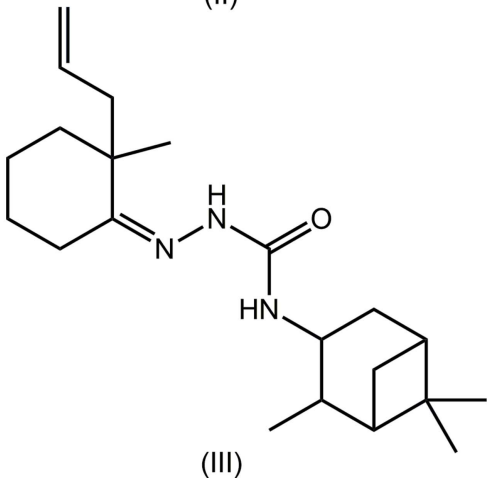

(III)

6. Synthesis and crystallization

Analytical grade reagents were used as procured without further purification. 4-Phenylsemicarbazide (1.51 g, 0.01 mol) and vanillylacetone (1.94 g, 0.01 mol) were dissolved separately in hot absolute ethanol (30 ml) and mixed with stirring. The reaction mixture was heated and stirred for 20 min., then stirred for another 30 min. at room temperature. The resulting white precipitate was filtered off, washed with cold absolute ethanol and dried *in vacuo*; yield: 75%. Light-yellow prisms of (I) were grown at room temperature from slow evaporation of mixed solvents of ethanol and acetonitrile (1:1; *v*/*v* 20 ml). IR (cm^{-1}): 3201 ν(N—H), 1670 ν(C═N), 1213 ν(C—N), 1026 ν(C═O). MS *m*/*z*: 327.25 $[M+1]^+$

Table 4
Experimental details.

Crystal data	
Chemical formula	$C_{18}H_{21}N_3O_3$
M_r	327.37
Crystal system, space group	Monoclinic, $P2_1/n$
Temperature (K)	100
a, *b*, *c* (Å)	16.5464 (4), 9.2184 (2), 22.3975 (4)
β (°)	100.494 (2)
V (Å^3)	3359.18 (13)
Z	8
Radiation type	Cu *Kα*
μ (mm^{-1})	0.73
Crystal size (mm)	0.25 × 0.16 × 0.06
Data collection	
Diffractometer	Oxford Diffraction Xcaliber Eos Gemini
Absorption correction	Multi-scan (*CrysAlis PRO*; Agilent, 2011)
T_{min}, T_{max}	0.917, 1.000
No. of measured, independent and observed [$I > 2\sigma(I)$] reflections	23815, 6481, 5581
R_{int}	0.019
(sin θ/λ)$_{max}$ (Å^{-1})	0.615
Refinement	
$R[F^2 > 2\sigma(F^2)]$, $wR(F^2)$, *S*	0.059, 0.180, 1.05
No. of reflections	6481
No. of parameters	455
No. of restraints	6
H-atom treatment	H atoms treated by a mixture of independent and constrained refinement
$\Delta\rho_{max}$, $\Delta\rho_{min}$ (e Å^{-3})	0.60, −0.26

Computer programs: *CrysAlis PRO* (Agilent, 2011), *SHELXS97* (Sheldrick, 2008), *SHELXL2014* (Sheldrick, 2015), *ORTEP-3 for Windows* (Farrugia, 2012), *DIAMOND* (Brandenburg, 2006) and *publCIF* (Westrip, 2010).

7. Refinement

Crystal data, data collection and structure refinement details are summarized in Table 4. The carbon-bound H atoms were placed in calculated positions (C—H = 0.95–0.99 Å) and were included in the refinement in the riding-model approximation, with U_{iso}(H) set to 1.2–1.5U_{eq}(C). The oxygen- and nitrogen-bound H atoms were located in a difference-Fourier map but were refined with distance restraints of O—H = 0.84±0.01 Å and N—H = 0.88±0.01 Å, and with U_{iso}(H) set to 1.5U_{eq}(O) and 1.2U_{eq}(N), respectively. The maximum and minimum residual electron density peaks of 0.60 and 0.26 e Å^{-3}, respectively, were located 0.95 and 0.75 Å from atoms H10*A* and H36*A*, respectively.

Acknowledgements

We thank the staff of the University of Malaya's X-ray diffraction laboratory for the data collection.

Funding information

The authors are grateful for the support from Sunway University (INT-PRO-2017–096), Universiti Putra Malaysia (UPM), under the research University Grant Scheme (RUGS Nos 9199834 and 9174000), and from the Malaysian Ministry of Science, Technology and Innovation (grant No. 09–02–04–0752-EA001).

References

Agilent (2011). *CrysAlis PRO*. Agilent Technologies, Yarnton, England.
Ali, S. M. M., Azad, M. A. K., Jesmin, M., Ahsan, S., Rahman, M. M., Khanam, J. A., Islam, M. N. & Shahriar, S. M. S. (2012). *Asian Pac. J. Trop. Biomed.* **2**, 438–442.
Behenna, D. C., Mohr, J. T., Sherden, N. H., Marinescu, S. C., Harned, A. M., Tani, K., Seto, M., Ma, S., Novák, Z., Krout, M. R., McFadden, R. M., Roizen, J. L., Enquist, J. A. Jr, White, D. E., Levine, S. R., Petrova, K. V., Iwashita, A., Virgil, S. C. & Stoltz, B. M. (2011). *Chem. Eur. J.* **17**, 14199–14223.
Beraldo, H. & Gambino, D. (2004). *Mini Rev. Med. Chem.* **4**, 31–39.
Brandenburg, K. (2006). *DIAMOND*. Crystal Impact GbR, Bonn, Germany.
Farrugia, L. J. (2012). *J. Appl. Cryst.* **45**, 849–854.
Groom, C. R., Bruno, I. J., Lightfoot, M. P. & Ward, S. C. (2016). *Acta Cryst.* B**72**, 171–179.
Groth, P. (1980). *Acta Chem. Scand.* A**34**, 609–620.
Hoek, W. G. M. van den, Bokkers, G., Krabbendam, H., Spek, A. L. & Kroon, J. (1980). *Z. Kristallogr.* **152**, 215–225.
Kıyak, B., Esenpınar, A. A. & Bulut, M. (2015). *Polyhedron*, **90**, 183–196.
Ma, S., Reeves, C. M., Craig, R. A. II & Stoltz, B. M. (2014). *Tetrahedron*, **70**, 4208–4212.
McKinnon, J. J., Jayatilaka, D. & Spackman, M. A. (2007). *Chem. Commun.* pp. 3814–3816.
Pandeya, S. N. (2012). *Acta Pharm.* **62**, 263–286.
Pandey, S. & Srivastava, R. S. (2010). *Lett. Drug. Des. Discov.* **7**, 694–706.
Sheldrick, G. M. (2008). *Acta Cryst.* A**64**, 112–122.
Sheldrick, G. M. (2015). *Acta Cryst.* C**71**, 3–8.
Spek, A. L. (2009). *Acta Cryst.* D**65**, 148–155.
Sriram, D., Yogeeswari, P. & Thirumurugan, R. (2004). *Bioorg. Med. Chem. Lett.* **14**, 3923–3924.
Tan, M. Y., Crouse, K. A., Ravoof, T. B., Jotani, M. M. & Tiekink, E. R. T. (2017). *Acta Cryst.* E**73**, 1001–1008.
Tan, M. Y., Crouse, K. A., Ravoof, T. B. S. A. & Tiekink, E. R. T. (2015). *Acta Cryst.* E**71**, o1047–o1048.
Westrip, S. P. (2010). *J. Appl. Cryst.* **43**, 920–925.

supporting information

Acta Cryst. (2018). E**74**, 21-27 [https://doi.org/10.1107/S2056989017017273]

3-{(*E*)-[4-(4-Hydroxy-3-methoxyphenyl)butan-2-ylidene]amino}-1-phenylurea: crystal structure and Hirshfeld surface analysis

Ming Yueh Tan, Karen A. Crouse, Thahira B. S. A. Ravoof, Mukesh M. Jotani and Edward R. T. Tiekink

Computing details

Data collection: *CrysAlis PRO* (Agilent, 2011); cell refinement: *CrysAlis PRO* (Agilent, 2011); data reduction: *CrysAlis PRO* (Agilent, 2011); program(s) used to solve structure: *SHELXS97* (Sheldrick, 2008); program(s) used to refine structure: *SHELXL2014* (Sheldrick, 2015); molecular graphics: *ORTEP-3 for Windows* (Farrugia, 2012) and *DIAMOND* (Brandenburg, 2006); software used to prepare material for publication: *publCIF* (Westrip, 2010).

3-{(*E*)-[4-(4-Hydroxy-3-methoxyphenyl)butan-2-ylidene]amino}-1-phenylurea

Crystal data

$C_{18}H_{21}N_3O_3$
$M_r = 327.37$
Monoclinic, $P2_1/n$
$a = 16.5464$ (4) Å
$b = 9.2184$ (2) Å
$c = 22.3975$ (4) Å
$\beta = 100.494$ (2)°
$V = 3359.18$ (13) Å^3
$Z = 8$
$F(000) = 1392$
$D_x = 1.295$ Mg m^{-3}
Cu $K\alpha$ radiation, $\lambda = 1.5418$ Å
Cell parameters from 9245 reflections
$\theta = 3.7$–71.3°
$\mu = 0.73$ mm^{-1}
$T = 100$ K
Prism (cut), light-yellow
0.25 × 0.16 × 0.06 mm

Data collection

Oxford Diffraction Xcaliber Eos Gemini diffractometer
Radiation source: fine-focus sealed tube
Graphite monochromator
Detector resolution: 16.1952 pixels mm^{-1}
ω scans
Absorption correction: multi-scan (CrysAlis PRO; Agilent, 2011)
$T_{min} = 0.917$, $T_{max} = 1.000$
23815 measured reflections
6481 independent reflections
5581 reflections with $I > 2\sigma(I)$
$R_{int} = 0.019$
$\theta_{max} = 71.4°$, $\theta_{min} = 3.7°$
$h = -20\rightarrow20$
$k = -11\rightarrow11$
$l = -26\rightarrow27$

Refinement

Refinement on F^2
Least-squares matrix: full
$R[F^2 > 2\sigma(F^2)] = 0.059$
$wR(F^2) = 0.180$
$S = 1.05$
6481 reflections
455 parameters
6 restraints
Hydrogen site location: mixed
H atoms treated by a mixture of independent and constrained refinement
$w = 1/[\sigma^2(F_o^2) + (0.1131P)^2 + 1.5134P]$ where $P = (F_o^2 + 2F_c^2)/3$
$(\Delta/\sigma)_{max} < 0.001$
$\Delta\rho_{max} = 0.60$ e Å^{-3}
$\Delta\rho_{min} = -0.26$ e Å^{-3}

Special details

Geometry. All esds (except the esd in the dihedral angle between two l.s. planes) are estimated using the full covariance matrix. The cell esds are taken into account individually in the estimation of esds in distances, angles and torsion angles; correlations between esds in cell parameters are only used when they are defined by crystal symmetry. An approximate (isotropic) treatment of cell esds is used for estimating esds involving l.s. planes.

Fractional atomic coordinates and isotropic or equivalent isotropic displacement parameters (Å²)

	x	*y*	*z*	U_{iso}*/U_{eq}
O1	0.50355 (7)	0.34300 (14)	0.28183 (6)	0.0292 (3)
O2	0.22012 (9)	0.87251 (16)	0.56672 (6)	0.0386 (4)
O3	0.09139 (8)	1.04987 (16)	0.54412 (6)	0.0350 (3)
H3O	0.1190 (15)	1.034 (3)	0.5787 (7)	0.053*
N1	0.40785 (9)	0.29389 (16)	0.34177 (6)	0.0253 (3)
H1N	0.3694 (10)	0.337 (2)	0.3564 (9)	0.030*
N2	0.40724 (9)	0.51144 (16)	0.29066 (7)	0.0256 (3)
H2N	0.4313 (12)	0.5727 (19)	0.2696 (8)	0.031*
N3	0.34334 (9)	0.55389 (17)	0.31934 (7)	0.0284 (3)
C1	0.44364 (10)	0.37902 (19)	0.30419 (7)	0.0238 (3)
C2	0.43316 (10)	0.15426 (19)	0.36316 (8)	0.0259 (4)
C3	0.47454 (13)	0.0593 (2)	0.33074 (9)	0.0360 (4)
H3	0.4884	0.0887	0.2932	0.043*
C4	0.49550 (13)	−0.0785 (2)	0.35355 (10)	0.0407 (5)
H4	0.5243	−0.1425	0.3316	0.049*
C5	0.47517 (13)	−0.1240 (2)	0.40757 (10)	0.0419 (5)
H5	0.4894	−0.2186	0.4227	0.050*
C6	0.43353 (14)	−0.0291 (2)	0.43949 (10)	0.0442 (5)
H6	0.4192	−0.0594	0.4768	0.053*
C7	0.41258 (13)	0.1094 (2)	0.41765 (9)	0.0368 (4)
H7	0.3842	0.1734	0.4400	0.044*
C8	0.29887 (11)	0.6607 (2)	0.29621 (8)	0.0297 (4)
C9	0.23057 (11)	0.7061 (2)	0.32858 (9)	0.0326 (4)
H9A	0.2323	0.6455	0.3653	0.039*
H9B	0.1769	0.6900	0.3016	0.039*
C10	0.23837 (13)	0.8663 (2)	0.34707 (9)	0.0355 (4)
H10A	0.2974	0.8905	0.3592	0.043*
H10B	0.2158	0.9266	0.3113	0.043*
C11	0.19461 (12)	0.9052 (2)	0.39874 (8)	0.0329 (4)
C12	0.22808 (13)	0.8620 (2)	0.45796 (9)	0.0367 (4)
H12	0.2757	0.8024	0.4650	0.044*
C13	0.19215 (12)	0.9056 (2)	0.50660 (8)	0.0307 (4)
C14	0.12349 (11)	0.99627 (19)	0.49664 (8)	0.0261 (4)
C15	0.08828 (11)	1.0335 (2)	0.43795 (9)	0.0302 (4)
H15	0.0400	1.0915	0.4307	0.036*
C16	0.12319 (11)	0.9866 (2)	0.38942 (8)	0.0322 (4)
H16	0.0976	1.0108	0.3492	0.039*
C17	0.31178 (11)	0.7458 (2)	0.24149 (8)	0.0329 (4)
H17A	0.3595	0.8096	0.2526	0.049*

H17B	0.2628	0.8043	0.2266	0.049*
H17C	0.3214	0.6788	0.2095	0.049*
C18	0.30011 (18)	0.8105 (4)	0.58127 (11)	0.0742 (10)
H18A	0.2995	0.7133	0.5635	0.111*
H18B	0.3167	0.8039	0.6255	0.111*
H18C	0.3393	0.8718	0.5648	0.111*
O4	0.99721 (7)	0.19097 (14)	0.27509 (6)	0.0296 (3)
O5	0.74121 (9)	−0.41262 (16)	0.57259 (6)	0.0389 (3)
O6	0.59792 (8)	−0.55085 (16)	0.54521 (6)	0.0355 (3)
H6O	0.6277 (14)	−0.547 (3)	0.5798 (7)	0.053*
N4	0.90978 (8)	0.23778 (16)	0.34148 (6)	0.0245 (3)
H4N	0.8743 (10)	0.198 (2)	0.3602 (8)	0.029*
N5	0.90487 (9)	0.02044 (16)	0.28954 (7)	0.0263 (3)
H5N	0.9267 (12)	−0.040 (2)	0.2668 (8)	0.032*
N6	0.84546 (9)	−0.02354 (17)	0.32229 (7)	0.0288 (3)
C19	0.94100 (10)	0.15314 (18)	0.30127 (7)	0.0230 (3)
C20	0.93614 (10)	0.37987 (19)	0.35945 (8)	0.0251 (4)
C21	0.96816 (12)	0.4747 (2)	0.32082 (8)	0.0309 (4)
H21	0.9735	0.4440	0.2812	0.037*
C22	0.99218 (12)	0.6136 (2)	0.34046 (9)	0.0350 (4)
H22	1.0146	0.6768	0.3142	0.042*
C23	0.98404 (12)	0.6617 (2)	0.39743 (9)	0.0367 (4)
H23	1.0006	0.7571	0.4104	0.044*
C24	0.95139 (13)	0.5686 (2)	0.43530 (9)	0.0384 (5)
H24	0.9451	0.6008	0.4745	0.046*
C25	0.92765 (12)	0.4282 (2)	0.41667 (8)	0.0331 (4)
H25	0.9056	0.3653	0.4432	0.040*
C26	0.79860 (11)	−0.1278 (2)	0.30028 (8)	0.0292 (4)
C27	0.73558 (11)	−0.1766 (2)	0.33697 (9)	0.0330 (4)
H27A	0.6797	−0.1593	0.3134	0.040*
H27B	0.7417	−0.1189	0.3748	0.040*
C28	0.74571 (13)	−0.3380 (2)	0.35290 (9)	0.0364 (4)
H28A	0.7238	−0.3958	0.3163	0.044*
H28B	0.8051	−0.3600	0.3645	0.044*
C29	0.70304 (12)	−0.3848 (2)	0.40393 (9)	0.0327 (4)
C30	0.74324 (12)	−0.3697 (2)	0.46427 (9)	0.0342 (4)
H30	0.7957	−0.3245	0.4729	0.041*
C31	0.70709 (12)	−0.4203 (2)	0.51172 (8)	0.0307 (4)
C32	0.63080 (11)	−0.49006 (19)	0.49940 (8)	0.0265 (4)
C33	0.58946 (11)	−0.5002 (2)	0.44001 (9)	0.0320 (4)
H33	0.5367	−0.5443	0.4314	0.038*
C34	0.62477 (12)	−0.4461 (2)	0.39286 (8)	0.0326 (4)
H34	0.5951	−0.4510	0.3524	0.039*
C35	0.80405 (11)	−0.2075 (2)	0.24253 (8)	0.0329 (4)
H35A	0.8160	−0.1383	0.2120	0.049*
H35B	0.7516	−0.2560	0.2274	0.049*
H35C	0.8481	−0.2799	0.2506	0.049*
C36	0.82787 (14)	−0.3844 (3)	0.58750 (10)	0.0481 (6)

H36A	0.8572	−0.4519	0.5652	0.072*
H36B	0.8468	−0.3976	0.6312	0.072*
H36C	0.8388	−0.2845	0.5762	0.072*

Atomic displacement parameters (Å²)

	U^{11}	U^{22}	U^{33}	U^{12}	U^{13}	U^{23}
O1	0.0302 (6)	0.0278 (6)	0.0345 (7)	0.0047 (5)	0.0187 (5)	0.0035 (5)
O2	0.0518 (8)	0.0411 (8)	0.0266 (7)	0.0180 (6)	0.0167 (6)	0.0056 (5)
O3	0.0351 (7)	0.0431 (8)	0.0304 (7)	0.0075 (6)	0.0154 (5)	−0.0057 (6)
N1	0.0276 (7)	0.0269 (7)	0.0248 (7)	0.0014 (6)	0.0136 (6)	−0.0006 (6)
N2	0.0257 (7)	0.0268 (7)	0.0281 (7)	0.0019 (6)	0.0153 (6)	0.0016 (6)
N3	0.0294 (7)	0.0313 (8)	0.0282 (8)	0.0033 (6)	0.0152 (6)	−0.0005 (6)
C1	0.0241 (8)	0.0256 (8)	0.0227 (8)	−0.0003 (6)	0.0073 (6)	−0.0015 (6)
C2	0.0271 (8)	0.0268 (9)	0.0245 (8)	−0.0036 (7)	0.0064 (6)	0.0007 (7)
C3	0.0475 (11)	0.0307 (10)	0.0352 (10)	0.0047 (8)	0.0222 (9)	0.0055 (8)
C4	0.0455 (11)	0.0308 (10)	0.0500 (12)	0.0066 (8)	0.0196 (9)	0.0071 (9)
C5	0.0435 (11)	0.0326 (10)	0.0498 (12)	−0.0010 (8)	0.0088 (9)	0.0140 (9)
C6	0.0571 (13)	0.0425 (12)	0.0363 (11)	−0.0079 (10)	0.0172 (9)	0.0121 (9)
C7	0.0463 (11)	0.0359 (10)	0.0320 (10)	−0.0043 (8)	0.0176 (8)	0.0001 (8)
C8	0.0296 (9)	0.0336 (9)	0.0277 (9)	0.0013 (7)	0.0097 (7)	−0.0028 (7)
C9	0.0283 (9)	0.0367 (10)	0.0353 (10)	0.0005 (7)	0.0123 (7)	−0.0034 (8)
C10	0.0449 (11)	0.0343 (10)	0.0314 (10)	0.0030 (8)	0.0179 (8)	0.0023 (8)
C11	0.0419 (10)	0.0292 (9)	0.0307 (9)	0.0023 (8)	0.0149 (8)	−0.0010 (7)
C12	0.0444 (11)	0.0351 (10)	0.0340 (10)	0.0142 (8)	0.0164 (8)	0.0035 (8)
C13	0.0395 (10)	0.0289 (9)	0.0265 (9)	0.0058 (7)	0.0134 (7)	0.0019 (7)
C14	0.0292 (9)	0.0239 (8)	0.0291 (9)	−0.0029 (6)	0.0163 (7)	−0.0021 (6)
C15	0.0246 (8)	0.0327 (9)	0.0354 (10)	0.0004 (7)	0.0110 (7)	0.0012 (7)
C16	0.0333 (9)	0.0384 (10)	0.0262 (9)	0.0011 (8)	0.0087 (7)	0.0005 (7)
C17	0.0342 (9)	0.0383 (10)	0.0289 (9)	0.0117 (8)	0.0133 (7)	0.0041 (7)
C18	0.0821 (19)	0.111 (3)	0.0325 (11)	0.0655 (19)	0.0182 (12)	0.0211 (13)
O4	0.0312 (6)	0.0265 (6)	0.0362 (7)	−0.0032 (5)	0.0200 (5)	−0.0031 (5)
O5	0.0459 (8)	0.0460 (8)	0.0266 (7)	−0.0145 (6)	0.0118 (6)	−0.0018 (6)
O6	0.0317 (7)	0.0471 (8)	0.0312 (7)	−0.0050 (6)	0.0152 (5)	0.0059 (6)
N4	0.0245 (7)	0.0272 (7)	0.0244 (7)	−0.0009 (5)	0.0116 (5)	0.0008 (5)
N5	0.0271 (7)	0.0279 (8)	0.0279 (7)	−0.0029 (6)	0.0159 (6)	−0.0030 (6)
N6	0.0296 (8)	0.0313 (8)	0.0296 (8)	−0.0042 (6)	0.0166 (6)	−0.0001 (6)
C19	0.0223 (8)	0.0250 (8)	0.0230 (8)	0.0008 (6)	0.0075 (6)	0.0015 (6)
C20	0.0223 (8)	0.0286 (9)	0.0249 (8)	0.0030 (6)	0.0057 (6)	−0.0027 (7)
C21	0.0371 (10)	0.0287 (9)	0.0297 (9)	−0.0013 (7)	0.0140 (7)	−0.0046 (7)
C22	0.0376 (10)	0.0287 (10)	0.0421 (11)	−0.0032 (8)	0.0162 (8)	−0.0037 (8)
C23	0.0379 (10)	0.0301 (10)	0.0431 (11)	0.0004 (8)	0.0104 (8)	−0.0121 (8)
C24	0.0458 (11)	0.0394 (11)	0.0313 (10)	0.0059 (9)	0.0103 (8)	−0.0108 (8)
C25	0.0384 (10)	0.0346 (10)	0.0286 (9)	0.0039 (8)	0.0125 (8)	−0.0005 (7)
C26	0.0275 (9)	0.0306 (9)	0.0311 (9)	−0.0004 (7)	0.0098 (7)	0.0036 (7)
C27	0.0293 (9)	0.0332 (10)	0.0395 (10)	−0.0004 (7)	0.0144 (8)	0.0038 (8)
C28	0.0450 (11)	0.0340 (10)	0.0345 (10)	0.0026 (8)	0.0186 (8)	0.0026 (8)
C29	0.0403 (10)	0.0281 (9)	0.0326 (10)	0.0010 (7)	0.0143 (8)	0.0029 (7)

C30	0.0373 (10)	0.0318 (10)	0.0361 (10)	−0.0073 (8)	0.0131 (8)	−0.0007 (8)
C31	0.0375 (10)	0.0296 (9)	0.0270 (9)	−0.0041 (7)	0.0111 (7)	−0.0026 (7)
C32	0.0288 (9)	0.0249 (8)	0.0299 (9)	0.0034 (7)	0.0165 (7)	0.0012 (7)
C33	0.0241 (8)	0.0377 (10)	0.0357 (10)	0.0035 (7)	0.0095 (7)	0.0007 (8)
C34	0.0341 (9)	0.0365 (10)	0.0280 (9)	0.0043 (8)	0.0077 (7)	0.0021 (7)
C35	0.0330 (9)	0.0400 (11)	0.0267 (9)	−0.0114 (8)	0.0076 (7)	−0.0018 (7)
C36	0.0474 (12)	0.0608 (15)	0.0358 (11)	−0.0236 (11)	0.0064 (9)	−0.0054 (10)

Geometric parameters (Å, º)

O1—C1	1.235 (2)	O4—C19	1.237 (2)
O2—C13	1.376 (2)	O5—C31	1.379 (2)
O2—C18	1.424 (3)	O5—C36	1.436 (2)
O3—C14	1.365 (2)	O6—C32	1.366 (2)
O3—H3O	0.838 (10)	O6—H6O	0.840 (10)
N1—C1	1.363 (2)	N4—C19	1.362 (2)
N1—C2	1.410 (2)	N4—C20	1.416 (2)
N1—H1N	0.862 (9)	N4—H4N	0.865 (9)
N2—C1	1.371 (2)	N5—C19	1.366 (2)
N2—N3	1.3895 (19)	N5—N6	1.3899 (19)
N2—H2N	0.876 (9)	N5—H5N	0.878 (9)
N3—C8	1.281 (2)	N6—C26	1.276 (2)
C2—C7	1.388 (2)	C20—C25	1.388 (2)
C2—C3	1.394 (3)	C20—C21	1.400 (3)
C3—C4	1.390 (3)	C21—C22	1.389 (3)
C3—H3	0.9500	C21—H21	0.9500
C4—C5	1.379 (3)	C22—C23	1.380 (3)
C4—H4	0.9500	C22—H22	0.9500
C5—C6	1.389 (3)	C23—C24	1.384 (3)
C5—H5	0.9500	C23—H23	0.9500
C6—C7	1.388 (3)	C24—C25	1.394 (3)
C6—H6	0.9500	C24—H24	0.9500
C7—H7	0.9500	C25—H25	0.9500
C8—C17	1.503 (2)	C26—C35	1.504 (3)
C8—C9	1.509 (2)	C26—C27	1.509 (2)
C9—C10	1.533 (3)	C27—C28	1.532 (3)
C9—H9A	0.9900	C27—H27A	0.9900
C9—H9B	0.9900	C27—H27B	0.9900
C10—C11	1.516 (2)	C28—C29	1.512 (2)
C10—H10A	0.9900	C28—H28A	0.9900
C10—H10B	0.9900	C28—H28B	0.9900
C11—C16	1.383 (3)	C29—C34	1.393 (3)
C11—C12	1.399 (3)	C29—C30	1.400 (3)
C12—C13	1.392 (2)	C30—C31	1.392 (3)
C12—H12	0.9500	C30—H30	0.9500
C13—C14	1.395 (3)	C31—C32	1.399 (3)
C14—C15	1.381 (3)	C32—C33	1.384 (3)
C15—C16	1.389 (3)	C33—C34	1.389 (3)

C15—H15	0.9500	C33—H33	0.9500
C16—H16	0.9500	C34—H34	0.9500
C17—H17A	0.9800	C35—H35A	0.9800
C17—H17B	0.9800	C35—H35B	0.9800
C17—H17C	0.9800	C35—H35C	0.9800
C18—H18A	0.9800	C36—H36A	0.9800
C18—H18B	0.9800	C36—H36B	0.9800
C18—H18C	0.9800	C36—H36C	0.9800

C13—O2—C18	116.47 (15)	C31—O5—C36	116.80 (15)
C14—O3—H3O	115 (2)	C32—O6—H6O	115 (2)
C1—N1—C2	126.87 (14)	C19—N4—C20	125.70 (14)
C1—N1—H1N	113.9 (15)	C19—N4—H4N	116.7 (15)
C2—N1—H1N	118.8 (15)	C20—N4—H4N	117.3 (14)
C1—N2—N3	119.30 (14)	C19—N5—N6	119.11 (14)
C1—N2—H2N	117.9 (14)	C19—N5—H5N	118.1 (14)
N3—N2—H2N	121.7 (14)	N6—N5—H5N	121.7 (15)
C8—N3—N2	117.32 (15)	C26—N6—N5	117.01 (15)
O1—C1—N1	124.55 (16)	O4—C19—N4	124.09 (15)
O1—C1—N2	120.18 (15)	O4—C19—N5	120.13 (15)
N1—C1—N2	115.26 (14)	N4—C19—N5	115.77 (14)
C7—C2—C3	119.56 (17)	C25—C20—C21	118.93 (17)
C7—C2—N1	117.72 (16)	C25—C20—N4	118.80 (16)
C3—C2—N1	122.67 (15)	C21—C20—N4	122.24 (15)
C4—C3—C2	119.74 (17)	C22—C21—C20	119.91 (17)
C4—C3—H3	120.1	C22—C21—H21	120.0
C2—C3—H3	120.1	C20—C21—H21	120.0
C5—C4—C3	121.05 (19)	C23—C22—C21	121.23 (18)
C5—C4—H4	119.5	C23—C22—H22	119.4
C3—C4—H4	119.5	C21—C22—H22	119.4
C4—C5—C6	118.92 (19)	C22—C23—C24	118.82 (18)
C4—C5—H5	120.5	C22—C23—H23	120.6
C6—C5—H5	120.5	C24—C23—H23	120.6
C7—C6—C5	120.86 (19)	C23—C24—C25	120.83 (18)
C7—C6—H6	119.6	C23—C24—H24	119.6
C5—C6—H6	119.6	C25—C24—H24	119.6
C6—C7—C2	119.87 (19)	C20—C25—C24	120.26 (18)
C6—C7—H7	120.1	C20—C25—H25	119.9
C2—C7—H7	120.1	C24—C25—H25	119.9
N3—C8—C17	125.06 (16)	N6—C26—C35	124.91 (16)
N3—C8—C9	116.39 (16)	N6—C26—C27	116.46 (16)
C17—C8—C9	118.50 (16)	C35—C26—C27	118.58 (16)
C8—C9—C10	111.32 (16)	C26—C27—C28	111.04 (15)
C8—C9—H9A	109.4	C26—C27—H27A	109.4
C10—C9—H9A	109.4	C28—C27—H27A	109.4
C8—C9—H9B	109.4	C26—C27—H27B	109.4
C10—C9—H9B	109.4	C28—C27—H27B	109.4
H9A—C9—H9B	108.0	H27A—C27—H27B	108.0

C11—C10—C9	113.94 (16)	C29—C28—C27	114.03 (16)
C11—C10—H10A	108.8	C29—C28—H28A	108.7
C9—C10—H10A	108.8	C27—C28—H28A	108.7
C11—C10—H10B	108.8	C29—C28—H28B	108.7
C9—C10—H10B	108.8	C27—C28—H28B	108.7
H10A—C10—H10B	107.7	H28A—C28—H28B	107.6
C16—C11—C12	118.52 (17)	C34—C29—C30	118.35 (17)
C16—C11—C10	121.80 (17)	C34—C29—C28	121.90 (18)
C12—C11—C10	119.66 (17)	C30—C29—C28	119.74 (17)
C13—C12—C11	120.53 (18)	C31—C30—C29	120.59 (17)
C13—C12—H12	119.7	C31—C30—H30	119.7
C11—C12—H12	119.7	C29—C30—H30	119.7
O2—C13—C12	125.91 (17)	O5—C31—C30	125.60 (17)
O2—C13—C14	114.09 (15)	O5—C31—C32	114.27 (16)
C12—C13—C14	119.94 (17)	C30—C31—C32	120.10 (17)
O3—C14—C15	119.68 (16)	O6—C32—C33	119.97 (16)
O3—C14—C13	120.88 (16)	O6—C32—C31	120.60 (16)
C15—C14—C13	119.44 (16)	C33—C32—C31	119.41 (16)
C14—C15—C16	120.25 (17)	C32—C33—C34	120.25 (17)
C14—C15—H15	119.9	C32—C33—H33	119.9
C16—C15—H15	119.9	C34—C33—H33	119.9
C11—C16—C15	121.08 (17)	C33—C34—C29	121.09 (17)
C11—C16—H16	119.5	C33—C34—H34	119.5
C15—C16—H16	119.5	C29—C34—H34	119.5
C8—C17—H17A	109.5	C26—C35—H35A	109.5
C8—C17—H17B	109.5	C26—C35—H35B	109.5
H17A—C17—H17B	109.5	H35A—C35—H35B	109.5
C8—C17—H17C	109.5	C26—C35—H35C	109.5
H17A—C17—H17C	109.5	H35A—C35—H35C	109.5
H17B—C17—H17C	109.5	H35B—C35—H35C	109.5
O2—C18—H18A	109.5	O5—C36—H36A	109.5
O2—C18—H18B	109.5	O5—C36—H36B	109.5
H18A—C18—H18B	109.5	H36A—C36—H36B	109.5
O2—C18—H18C	109.5	O5—C36—H36C	109.5
H18A—C18—H18C	109.5	H36A—C36—H36C	109.5
H18B—C18—H18C	109.5	H36B—C36—H36C	109.5

C1—N2—N3—C8	−164.49 (16)	C19—N5—N6—C26	162.35 (16)
C2—N1—C1—O1	2.0 (3)	C20—N4—C19—O4	0.0 (3)
C2—N1—C1—N2	−179.42 (15)	C20—N4—C19—N5	−178.54 (15)
N3—N2—C1—O1	−175.81 (15)	N6—N5—C19—O4	175.95 (15)
N3—N2—C1—N1	5.6 (2)	N6—N5—C19—N4	−5.5 (2)
C1—N1—C2—C7	154.49 (18)	C19—N4—C20—C25	−151.84 (17)
C1—N1—C2—C3	−28.1 (3)	C19—N4—C20—C21	30.1 (3)
C7—C2—C3—C4	−0.7 (3)	C25—C20—C21—C22	1.1 (3)
N1—C2—C3—C4	−178.00 (18)	N4—C20—C21—C22	179.19 (17)
C2—C3—C4—C5	0.8 (3)	C20—C21—C22—C23	−1.0 (3)
C3—C4—C5—C6	−0.4 (3)	C21—C22—C23—C24	0.1 (3)

C4—C5—C6—C7	0.0 (3)	C22—C23—C24—C25	0.5 (3)
C5—C6—C7—C2	0.2 (3)	C21—C20—C25—C24	−0.5 (3)
C3—C2—C7—C6	0.2 (3)	N4—C20—C25—C24	−178.64 (16)
N1—C2—C7—C6	177.68 (18)	C23—C24—C25—C20	−0.3 (3)
N2—N3—C8—C17	−1.6 (3)	N5—N6—C26—C35	1.1 (3)
N2—N3—C8—C9	−179.23 (15)	N5—N6—C26—C27	178.73 (15)
N3—C8—C9—C10	123.12 (19)	N6—C26—C27—C28	−122.47 (19)
C17—C8—C9—C10	−54.7 (2)	C35—C26—C27—C28	55.3 (2)
C8—C9—C10—C11	−157.88 (16)	C26—C27—C28—C29	162.93 (17)
C9—C10—C11—C16	−108.0 (2)	C27—C28—C29—C34	95.8 (2)
C9—C10—C11—C12	73.9 (2)	C27—C28—C29—C30	−85.6 (2)
C16—C11—C12—C13	−2.8 (3)	C34—C29—C30—C31	2.6 (3)
C10—C11—C12—C13	175.28 (18)	C28—C29—C30—C31	−176.05 (18)
C18—O2—C13—C12	11.7 (3)	C36—O5—C31—C30	−16.5 (3)
C18—O2—C13—C14	−165.4 (2)	C36—O5—C31—C32	161.41 (18)
C11—C12—C13—O2	−178.72 (19)	C29—C30—C31—O5	179.33 (18)
C11—C12—C13—C14	−1.7 (3)	C29—C30—C31—C32	1.5 (3)
O2—C13—C14—O3	2.7 (3)	O5—C31—C32—O6	−3.6 (3)
C12—C13—C14—O3	−174.61 (17)	C30—C31—C32—O6	174.50 (17)
O2—C13—C14—C15	−178.04 (16)	O5—C31—C32—C33	177.97 (16)
C12—C13—C14—C15	4.6 (3)	C30—C31—C32—C33	−4.0 (3)
O3—C14—C15—C16	176.25 (16)	O6—C32—C33—C34	−176.20 (17)
C13—C14—C15—C16	−3.0 (3)	C31—C32—C33—C34	2.3 (3)
C12—C11—C16—C15	4.5 (3)	C32—C33—C34—C29	1.9 (3)
C10—C11—C16—C15	−173.55 (18)	C30—C29—C34—C33	−4.4 (3)
C14—C15—C16—C11	−1.6 (3)	C28—C29—C34—C33	174.28 (18)

Hydrogen-bond geometry (Å, º)

Cg1, Cg2 and Cg3 are the centroids of the C2–C7, C29–C34 and C20–C25 rings, respectively.

D—H···*A*	*D*—H	H···*A*	*D*···*A*	*D*—H···*A*
N1—H1*N*···N3	0.86 (2)	2.18 (2)	2.635 (2)	113 (2)
N4—H4*N*···N6	0.86 (2)	2.23 (2)	2.637 (2)	109 (1)
O3—H3*O*···O2	0.84 (2)	2.29 (3)	2.660 (2)	107 (2)
O6—H6*O*···O5	0.84 (2)	2.28 (2)	2.663 (2)	108 (2)
O3—H3*O*···N6^{i}	0.84 (2)	2.19 (2)	2.994 (2)	161 (2)
O6—H6*O*···N3^{ii}	0.84 (2)	2.22 (2)	3.013 (2)	157 (2)
N2—H2*N*···O4^{iii}	0.88 (2)	2.01 (2)	2.873 (2)	170 (2)
N4—H4*N*···O2^{i}	0.86 (2)	2.54 (2)	3.390 (2)	167 (2)
N5—H5*N*···O1^{iv}	0.88 (2)	2.04 (2)	2.900 (2)	169 (2)
C33—H33···O6^{v}	0.95	2.54	3.212 (2)	128
C15—H15···O3^{vi}	0.95	2.63	3.166 (2)	113
C33—H33···O6^{i}	0.95	2.54	3.212 (2)	128
C10—H10*A*···*Cg*1^{vii}	0.99	2.80	3.774 (2)	168

C18—H18*A*···*Cg*2^{ii}	0.98	2.66	3.603 (4)	161
C28—H28*B*···*Cg*3^{viii}	0.99	2.75	3.720 (2)	166

Symmetry codes: (i) −*x*+1, −*y*+1, −*z*+1; (ii) −*x*+1, −*y*, −*z*+1; (iii) −*x*+3/2, *y*+1/2, −*z*+1/2; (iv) −*x*+3/2, *y*−1/2, −*z*+1/2; (v) −*x*+1, −*y*−1, −*z*+1; (vi) −*x*, −*y*+2, −*z*; (vii) *x*, *y*+1, *z*; (viii) *x*, *y*−1, *z*.